Zeitschrift Kunststofftechnik
Journal of Plastics Technology

Wissenschaftlicher Arbeitskreis der Universitäts-Professoren der Kunststofftechnik

archival, peer-reviewed online Journal of the Scientific Alliance of Polymer Technology
archivierte, peer-rezensierte Internetzeitschrift des Wissenschaftlichen Arbeitskreises Kunststofftechnik (WAK)
www.plasticseng.com, www.kunststofftech.com

handed in/eingereicht: 07.04.2010
accepted/angenommen: 07.07.2010

Prof. Barbara O. Calcagno[1,2], Prof. Dr. Roderic Lakes[2], Prof. Dr. Tim Osswald[2], Prof. Dr. Wendy Crone[2]

[1]University of Puerto Rico, Mayagüez, [2]University of Wisconsin, Madison

Comparison of viscoplastic Properties for Polycarbonate, Polypropylene, and High Density Polyethylene

The viscoplastic behavior of high density polyethylene, polypropylene, and polycarbonate under uniaxial tensile loading at constant strain rate and large strains was studied. Standard ASTM samples of the polymers cast by injection molding were tested at room temperature and constant crosshead speed; testing was conducted in the range of 5 to 300 mm/min. A single constitutive relation which captures the plastic flow behavior of all three polymers was found as a function of strain and strain rate in the range of 0.01 to 0.1 s^{-1}*. The values of the model parameters for each polymer are presented. A relation for the yielding of the polymeric materials as a function of strain rate is also reported.*

Vergleich des viskoplastischen Verhaltens von Polycarbonat, Polypropylen und HD-Polyethylen

Das viskoplastische Verhalten von HD-Polyethylen, Polypropylen und Polycarbonat wurde unter einachsiger Zugbeanspruchung bei konstanter Dehngeschwindigkeit und großen Verformungen untersucht. Im Spritzgießverfahren wurden Standardproben nach ASTM hergestellt und bei Raumtemperatur und konstanter Abzugsgeschwindigkeit geprüft; die Geschwindigkeit wurde zwischen 5 und 300 mm/min variiert. Es konnte gezeigt werden, dass eine einzige Zustandsgleichung als Funktion der Dehnung und der Dehngeschwindigkeit im Bereich von 0,01 bis 0,1 s^{-1}*das Fließverhalten aller drei Kunststoffe abbildet. Die Modellgrößen für jeden einzelnen Kunststoff werden vorgestellt. Darüber hinaus konnte das Fließen der Materialien als Funktion der Dehngeschwindigkeit ermittelt werden.*

Comparison of Viscoplastic Properties for Polycarbonate, Polypropylene and High Density Polyethylene

B. Calcagno, R. Lakes, T. Osswald, W. Crone

The polymers investigated in this study, commonly processed by injection molding, are used in a wide range of industrial and household applications. Polypropylene (PP) and high-density polyethylene (HDPE) are semi-crystalline polymers widely used in applications such as packaging, coatings, thin-wall applications, non-woven fabrics, composite materials, and house and automobile functional parts [1-3]. HDPE is a tough polymer with low strength and stiffness, and high elongation at break; also less dense than other polymers. PP exhibits high dynamic loading capacity, and a higher strength and stiffness than HDPE. Polycarbonate (PC) is a transparent amorphous polymer with a high strength and stiffness, a great resistance to impact, and susceptible to crack under stress [2]. It is widely used in components in electrical and electronics applications, automotive industry, and in applications designed to resist impact such as helmets, body armors, windows, and eyeglasses [2, 4]. Given their widespread use, these materials warrant further study, particularly in the viscoplastic regime.

In general the properties of polymers vary depending upon the molecular structure, molecular weight, and crystallinity. Their mechanical properties are sensitive to variations in the temperature and the way the load is applied [5-7]. During tensile or compressive loading, many polymers deform viscoelastically, yield, and eventually exhibit viscoplastic deformation before failure. The yielding and post yielding phenomena with neck formation and its subsequent propagation during cold drawing depend heavily on the strain rate [8-12]. The post yielding is generally accompanied by strain softening and cold drawing by strain hardening at large strains [13, 14].

Viscoplastic behavior occurs under certain loading conditions and is a well-defined part of the failure process. When a material under an applied stress deforms as ideal elastic solid, the stress and the strain response are linearly proportional and in phase. If the material is a liquid, the stress is proportional to the strain rate, and the stress and the strain are out of phase. Polymers exhibit the characteristic behavior between elastic solid and a liquid. In the viscoelastic range, their behavior has been modeled, and their viscoelastic properties measured experimentally performing dynamic mechanical measurements [15, 16]. If the stress applied continues to increase the polymers will yield at a maximum stress known as the yield stress and fracture will occur for brittle polymers. For some ductile polymers plastic deformation occurs with stable necking and cold drawing with strain hardening, while for others unstable necking will end in fracture [15]. The extent of cold drawing observed is dependent on the polymer and loading conditions.

In general, viscoplasticity occurs during the post yielding and cold drawing processes, following elastic deformation and necking. An appreciable load drop is observed after yielding and the cold drawing process occurs at a nominally constant load with the cold drawn cross section remaining relatively constant [9, 17]. Significant morphological changes occur throughout the cold drawing process. At large strains, cavitation and phase transformation can be present. The first deformation mechanism in a semicrystalline polymer under a uniaxial tensile load is the extension of the molecules in the amorphous phase, followed by alignment and orientation of the lamellae contained in the spherulitic structure, and crazing which consists of stretching of the fibrils/microfibrils and nucleation of voids [7, 9, 18-20]. The fibrilar structure is responsible for the strain hardening at large deformations. Glassy polymers have a random distribution of their molecule chain lengths. They yield under load exhibiting nucleation and growth of localized shear bands inclined along the axis of loading. These shear bands propagate along the gauge length of the specimen producing a homogeneous strain hardening of the polymer [21-23].

Compression, tensile, and shear tests are commonly used to characterize solid-state rheology of polymers [12, 13, 24-28]. Several constitutive relations that describe the viscoplastic behavior of solid polymers have been obtained for different strains and strain rates ranges, and temperatures. Some of them relate true stresses and strains calculated from the nominal values, while others have been performed using different techniques to measure the true stress and strain. An overview of relevant experimental results and constitutive models is presented below.

1 BACKGROUND

A number of investigators have carried out experimental testing to characterize the viscoplastic behavior of polymers. Although the comparative study reported in the Results below focuses on polycarbonate (PC), polypropylene (PP), and high density polyethylene (HDPE), prior tensile testing results published on these and other polymers are also valuable for comparison. Several of their prior works were done at constant true strain rate using different techniques, while others used constant crosshead speed to apply the load to the samples. A wide variety of strain rates, temperatures, and ways of loading were used to investigate the plastic deformation of different polymers. Some of the most relevant of these prior works on PC are considered first.

The viscoplastic behavior of PC and many other amorphous polymers have been studied using traditional uniaxial tension and compression, torsion and simple shear tests. For very high strain rates, split Hopkinson bars in tension [10], compression [29-31] and torsion [23] have been used.

G'Sell and Gopez [21] investigated PC in plane simple shear at several temperatures and shear rates and developed a constitutive equation for steady state plasticity up to shear strains of 2.0. A three-dimensional constitutive model based on the macromolecular structure and the micromechanism of plastic flow was developed by Boyce et al [32] and used to model poly(methylmethacrylate) (PMMA) tensile behavior at large deformations. Boyce and Arruda [11] applied the same model to analyze the plastic flow of PC in compression at strain rates ranging from 1.0 s^{-1} to 0.0001 s^{-1}, and in tension at crosshead speeds ranging from 1.27 mm/min to 12.7 mm/min.

Duan et al [14] proposed a uniform constitutive model to predict the behavior of glassy and semicrystalline polymers under compressive load as a function of true strain, true strain rate, and temperature at low strain rates. Mulliken and Boyce [4] performed a theoretical and experimental to study the rate dependent behavior of PC and PMMA under strain rates ranging from 10^{-4} to 10^{4} s^{-1} using uniaxial compression tests on a servohydraulic machine and the split-Hopkinson bar. Sarva et al [10] used the constitutive model derived by Mulliken and Boyce to study and simulate the deformation of PC during tensile loading at nominal strain rates of 500 to 1500 s^{-1} using a split collar type Hopkinson tension bar.

G'Sell and Jonas [26] carried out tensile tension tests at constant true strain rate between 10^{-4} and 10^{-1} s^{-1} with a diametral transducer, an exponential function generator, and a closed loop hydraulic machine on poly(vinyl chloride) (PVC), and high density polyethylene (HDPE). They determined the following constitutive equation to describe their flow stress behavior:

$$\sigma = K \exp\left[\left(\frac{\gamma_e}{2}\right)\varepsilon^2\right]\dot{\varepsilon}^m$$

where K and γ_e are constants, m the strain rate sensitivity, ε and $\dot{\varepsilon}$ the true strain and true strain rate. Using the same technique to control the local true strain rate, G'Sell and Jonas [33] carried out tensile tension tests at constant and transient true strain rate on several semicrystalline and glassy polymers. They observed a true yield drop in the glassy polymers while the semicrystalline exhibited a gradual yielding. They proposed a model based on the dynamics of plastic waves to explain the difference of transient behavior of the polymers investigated when the strain increased. The strain rate ranged from 10^{-4} to 10^{-1} s^{-1}. The previous testing technique was modified by G'Sell et al [34] and used to test hour-glass-shaped samples of several polymers and reported in detail the results for HDPE and polycarbonate (PC) at selected strain rates between $5x10^{-5}$ to 10^{-3} s^{-1} at 25°C.

Drozdov and Cristiansen [12, 35] derived constitutive equations for the viscoelastic and viscoplastic behavior of HDPE tested in tensile tests at constant strain rates and relaxation tests at temperatures ranging from 25°C to 90°C and small strains (up to $\varepsilon = 0.4$). The polymer was modeled as a heterogeneous, incompressible, and transient network of chains bridged by junctions, and the parameters were found by fitting the experimental data.

Furthermore, several papers have reported studies performed on PP using true strain rates and also constant crosshead speed. Duffo and G'Sell [13] investigated the behavior of isotactic polypropylene (PP) under tensile tests where true strain rate on the deforming neck was regulated with a video-controlled testing system in a range of temperatures from 20° to 150°C. The strain rates varied between 10^{-5} to 10^{-3} s^{-1}. They used the following multiplicative relation between the effective stress and strain:

$$\sigma(\varepsilon, \dot{\varepsilon}) = k[1 - \exp(-w\varepsilon)]\exp(h\varepsilon^2)\left(\frac{\dot{\varepsilon}}{\dot{\varepsilon}_o}\right)^m$$

where ε and $\dot{\varepsilon}$ are the strain and strain rate, k the scaling factor, w the viscoelastic coefficient, h the strain-hardening parameter, and m the strain-rate sensitivity coefficient. This constitutive equation was used to predict the development of stretching instabilities of PP at different temperatures.

The yielding and post-yielding behavior of PP has been studied by Kontou et al [36], using dogbone shape tensile specimens for the tension tests, and cylindrical specimens for the compressive tests. The tests were performed at 0.1, 1, and 10 mm/min. A laser-extensometer system was used to measure the true elongation and strain rates, and a nonlinear viscoelastic constitutive model was implemented to describe the behavior observed for the strain rates tested. Spathis and Kontou [37] modified a plasticity theory developed to describe the plastic deformation of metals to predict the true stress-strain curves of semicrystalline polymers using the same non-contact measurement method and crosshead speeds. They incorporated entropic hardening terms to account for the strain hardening effect and a scaling rule of non-linear viscoelasticity to describe the rate effect of yielding. The model was validated with tensile experiments done on PP.

Drozdov and Christiansen [1, 27] performed uniaxial tensile tests on isotactic PP with constants strain rates ranging from 5 to 200 mm/min at finite strains. The viscoplastic behavior of the polymer was modeled using an equivalent heterogeneous network of chains bridged by permanent junctions and used to assess the influence of strain rate and thermal pre-treatment on isotactic PP at strains below the onset of necking.

A comparative study by Dasari et al [9] on the strain rate sensitivity index and microstructure evolution was published on HDPE, homopolymer PP, and isotactic PP tested in tension at selected constant strain rates between 0.25 and 380 mm/min. Sections of the samples were analyzed after different stages of plastic deformation were attained, and the microstructures observed were correlated with the deformation and fracture processes. They reported a single linear increase in yield stress with increase in strain rate that follows Eyring's equation. HDPE exhibited a higher resistance to necking and greater susceptibility to plastic deformation (corresponding to higher strain rate sensitivity index) followed by PP, and iPP in both, low and high strain regimes. During plastic deformation of HDPE in the low strain regime (at all strain rates) wedges and ridges appeared and increased, followed by crazing in the high strain regime. At low displacement rates the fracture of HDPE was ductile, characterized by fibrillation while at high strain rates, a mixture of fibrillation and crazing occurred lowering its toughness and ductility. On the other hand, PP and iPP, strain whitening and crazing occurred for both strain regimes without wedges and ridges mode of deformation. Fracture occurred by crazing-tearing mode in a more brittle manner compared to HDPE.

In the work reported below, the plastic flow of two semicrystalline polymers, PP, and HDPE, and one glassy polymer, PC under uniaxial tensile loading to large strains (up to 500 percent) was investigated to find a constitutive equation $\sigma(\varepsilon,\dot{\varepsilon})$ to represent the plastic deformation of the three polymeric materials investigated as a function of strain and strain rate. Standard ASTM tensile bars of the polymers were cast by injection molding process, and tested at room temperature over a range of constant crosshead speed. The results obtained were modeled to develop a constitutive relation following Eyring's equation for yielding and a unique relation to describe the viscoplastic behavior for all three polymers studied.

2 MATERIALS AND EXPERIMENTAL METHOD

The polymers investigated in this study were: polypropylene (PP), polycarbonate (PC), and high density polyethylene (HDPE) in sheets 1/16" thick from McMaster (#8742K131, #8574K24, #8619K421). Melting Flow Index (MFI) tests were performed on the PC, PP, and the HDPE samples following the ASTM D1238 [38]. The MFI test measures the rate of extrusion of a melted polymer trough a die under prescribed conditions of temperature, load, piston weight, diameter, and length of the die. The melt flow index is the weight of the polymer in grams extruded during 10 minutes [3]. The values obtained were 10.35 for PC, 0.53 for PP, and 0.34 for HDPE.

The sheets of polymers were shredded into small pieces. The PC was pre-dried [39] in the furnace at 124°C for 6 hours and stored in a vacuum container.

Tensile bars with the dimensions of Type I specified in ASTM D 638 were cast by using injection-molding process (see Figure 1).

The temperatures used in the melting zone of the injection-molding machine (BOY 22S, Dipronic) were the following: 216°C for PP, 280°C for PC, and 185°C for HDPE.

Uniaxial tension tests were carried out at room temperature (19.5°C ± 0.5°C) on a servo-hydraulic testing machine, an Instron 5566 and following the ASTM D-

638 [40] standard. The data acquisition during the tests was done using the Merlin software. The dogbone shaped specimens were placed between two grips, one of them fixed and the other moving at a programmed constant crosshead speed between 5 to 300 mm/min. The tests ended when the sample fractured or reached a maximum stretch of 5.

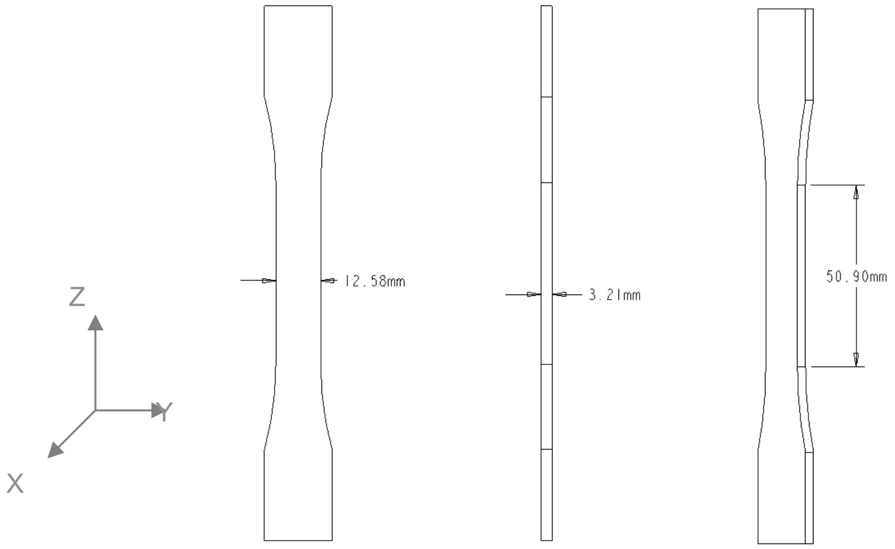

Figure 1: Tensile samples geometry and dimensions

The nominal stresses, σ_{zz}^{N}, were calculated using the ratio between the forces measured by the load cell and the initial cross section area. The nominal strain, ε_{ZZ}, was calculated using the displacement of the upper grip divided by the initial gage length (50 mm). For the true stresses, σ_{ZZ}^{True}, the polymers were assumed incompressible and the following equation was used:

$$\sigma_{ZZ}^{True} = \sigma_{zz}^{N}(1+\varepsilon_{ZZ}) \quad (1)$$

For the samples that showed cold drawing, the cold drawing stress, σ_{CD}, was calculated using the load divided by the final cross section area of the sample neck.

$$\sigma_{CD} = \frac{F}{A_{final}} \quad (2)$$

The graphs that display the relationship between the stress and crosshead speed at constant strain were constructed using the plots of stress vs. strain obtained at a fixed crosshead speed. For a chosen strain, and crosshead speed the stress was found by linear interpolation.

A multivariable non-linear least square fitting (NLSF) using Origin 7.5 software was performed to fit the data obtained for each polymer. Several relations were attempted to correlate the stress as the dependent variable and the strain and strain rate as the independent variables. The strain rates were calculated using the crosshead speed and the initial gage length.

3 RESULTS

Engineering stress-strain curves were plotted for all polymers and strain rates tested. All curves show an elastic region, where the stresses vary linearly with strain, a peak corresponding to the yield point, a post-yielding region with a sharp decrease in stress, and a cold-drawing region where the neck propagates steadily along the sample. Figures 2, 3, and 4 display the response of the three polymers at several selected crosshead speeds. The plot for PC in Figure 2 shows almost no change in the nominal stresses in the pre-yield region with increase of the crosshead speeds.

The yield strength increased up to 8% when the crosshead speed went from 5 mm/min to 300 mm/min. This behavior is observed also in the post-yield region. The stresses during the cold drawing region increased steadily until fracture occurred. The maximum strain attained was close to 2.5 and even for the highest speed tested, the samples displayed stable necking.

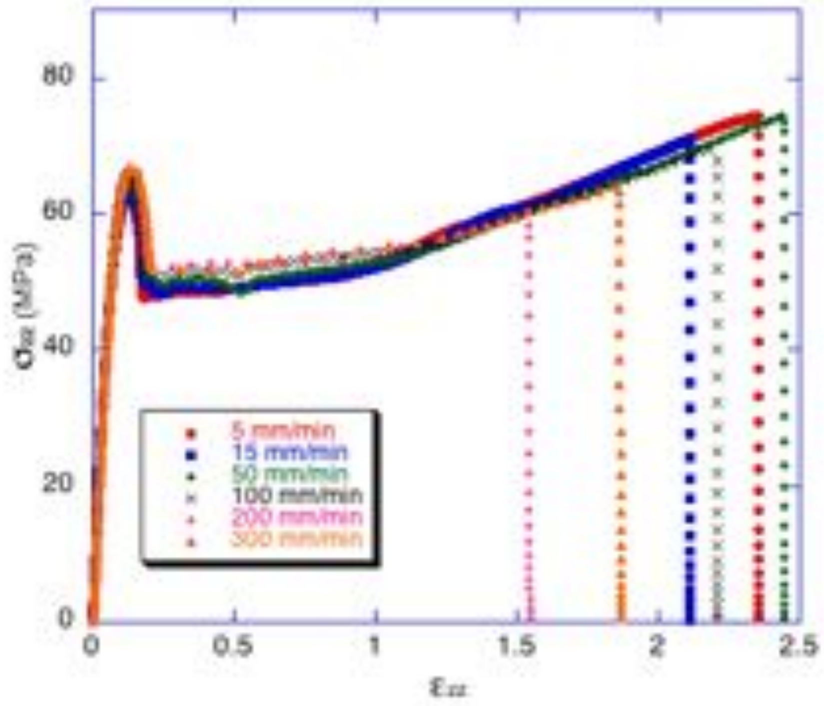

Figure 2: Nominal stress vs. strain for polycarbonate at selected crosshead speeds

The PP was tested at strain rates that varied from 10 mm/min to 300 mm/min. Over this range the yield strength increased 25%. For low crosshead speeds the cold drawing region extended in some cases up to strains equal to 5.5. In general, as the crosshead speed increased, the elongation of the neck at fracture, decreased. For strain rates equal or greater to 75 mm/min, the samples fracture after a very short neck or almost no necking (see Figure 3).

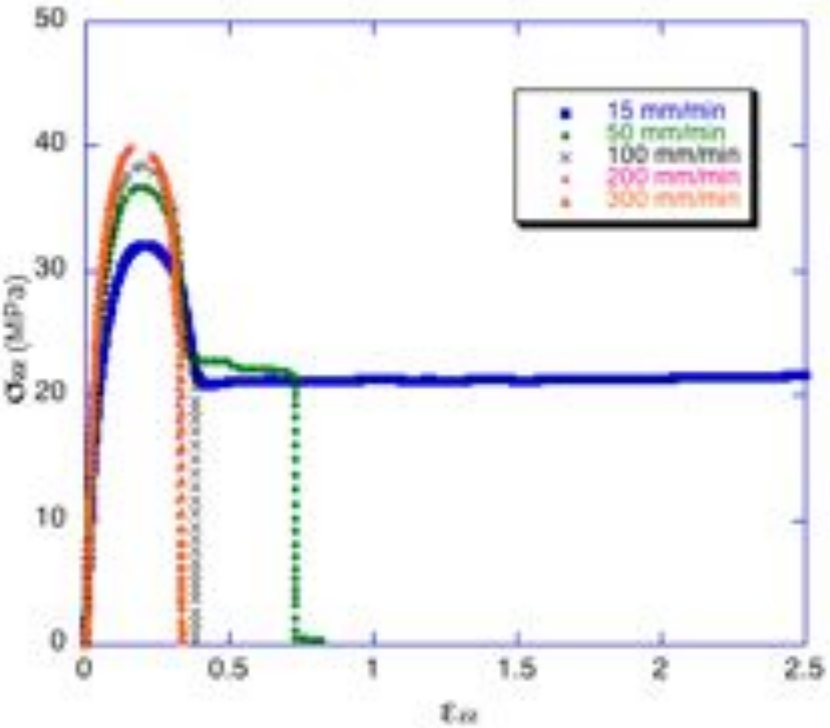

Figure 3: Nominal stress vs. strain for polypropylene at selected crosshead speeds

Figure 4 shows that the HDPE samples behaved similarly to the PP samples but with strain at fracture smaller than 300%. The increase of yield strength with strain rates was the largest of the three polymers tested, close to 30%. The stress during the propagation of the neck for each strain rate was approximately constant until failing occurred.

During plastic deformation of the PP and HDPE whitening of the region where necking occurred and propagation over the entire sample was observed. This effect is attributed to the separation and fragmentation of the crystalline lamellae, followed by rearrangement into a fibrillar structure [7, 9, 13, 17]. PC samples remained clear during the process.

Figure 5 displays the necking and plastic deformation of the three polymers during a tensile test at a crosshead speed of 25 mm/min. During the tests the images were captured with a Pixelink camera model #PL-A662 at 1 frame per second. All the times were measured from the starting of the test.

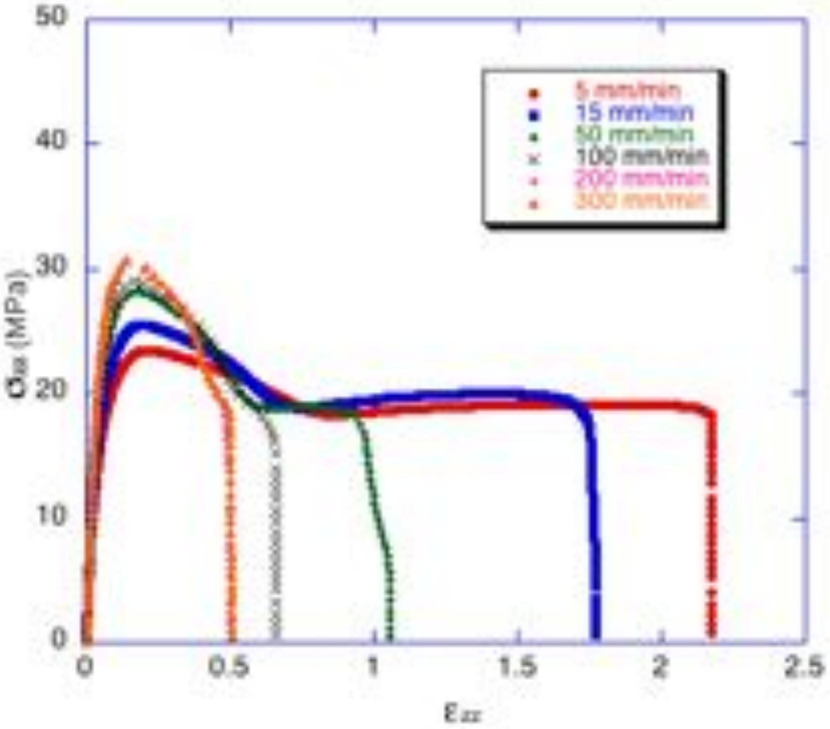

Figure 4: Nominal stress vs. strain for high density polyethylene at selected crosshead speeds

For the PP sample, image a was captured after 1 second the test started, in image b, at 4 seconds, slight whitening of the sample is observed which it is intensified and propagated to the whole sample in image c taken at 7 seconds. Image d (9 seconds) depicts the initiation of the necking, which occurred for all the samples in the first segment of the narrow region close to the pressure sensor. Images e and f (9 and 11 seconds) show the development of the neck until the cross section is constant and the neck propagates along the sample as it is depicted in image g taken at 16 seconds. At this point the strain corresponds to the natural draw ratio of the polymer and the nominal stress reaches a minimum as it is displayed in Figure 3 for PP.

The HDPE follows the same deformation pattern of the PP although with a different neck shape development. The images shown were captured at 1, 8, 9, 11, 13, 16 and 19 seconds. Although the HDPE samples are translucent initially, whitening is observed to occur in the region were the necking starts (image c) and the necking region propagates slower than the PP along the sample as images e, d, and f show. During the cold drawing event, which starts in image g, the cross sectional area decreases slightly until the sample fails.

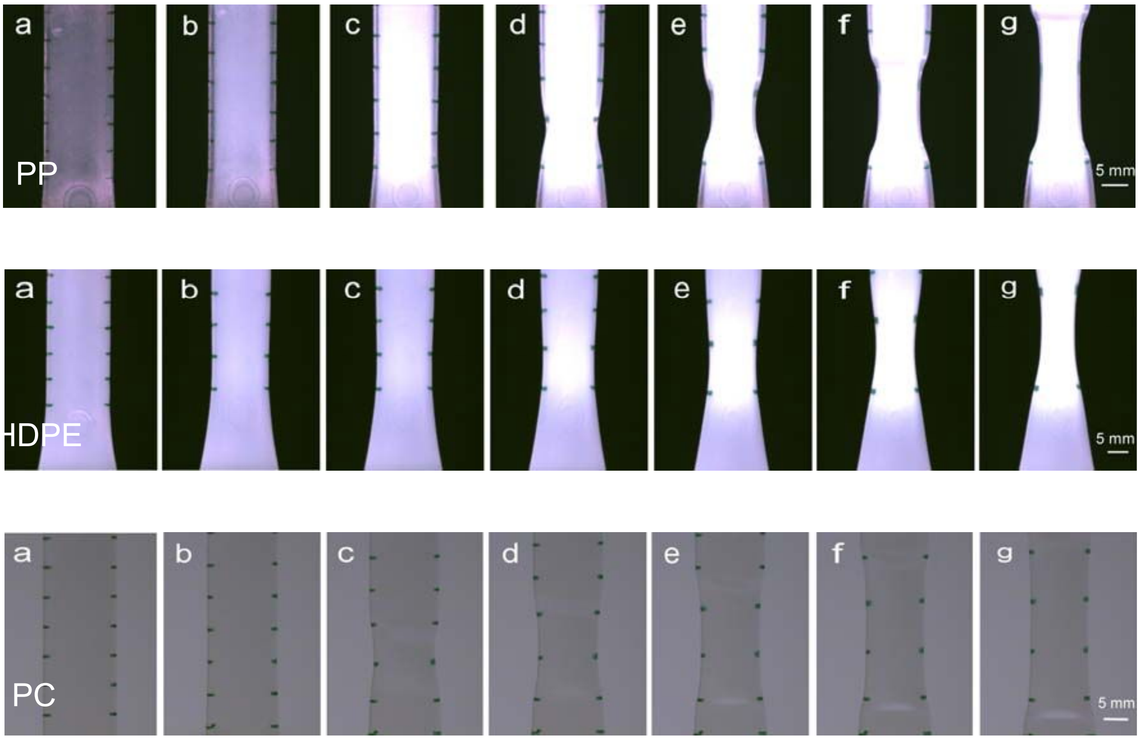

Figure 5: Sequence of pictures showing the deformation process of PP, HDPE, and PC during tensile tests performed at 25 mm/min.

The images were captured at the following times: 1, 4, 7, 9, 11, 13, and 16 seconds, for the PP; 1, 8, 9, 11, 13, 16, and 19 seconds, for the HDPE; 1, 5, 6, 7, 8, 9, and 10 seconds, for the PC. All the times are measured from the beginning of the test.

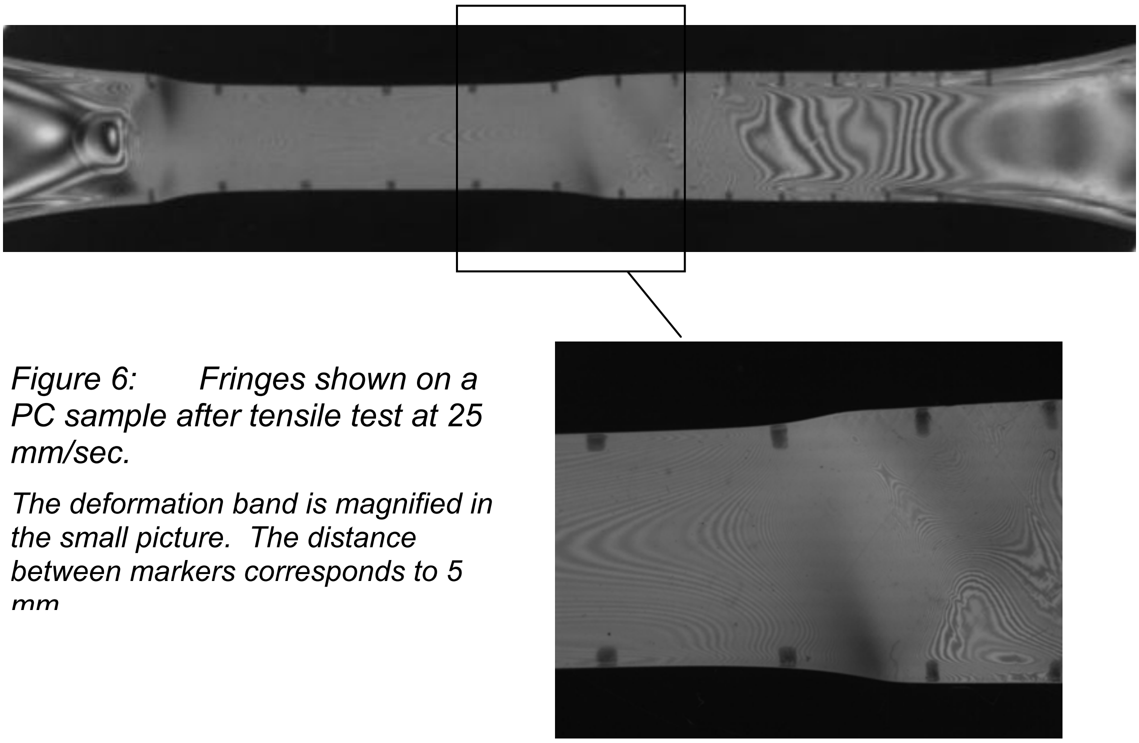

Figure 6: Fringes shown on a PC sample after tensile test at 25 mm/sec.

The deformation band is magnified in the small picture. The distance between markers corresponds to 5 mm

For the PC sample the pictures shown correspond to 1, 5, 6, 7, 8, 9, and 10 seconds. Image c depicts the start of the necking with the appearance of a deformation band, which occurred for all the samples between the second and third segment of the narrow region close to the pressure sensor. The rest of the images show a quick formation of a stable neck. The cross section keeps constant while the neck propagates along the whole sample while the nominal stress increases steadily as Figure 2 shows. Figure 6 shows the fringes captured on the birefringent PC sample when viewing the sample between two sheets of polarizing film. Although not analyzed in detail, the image in Figure 6 (bottom) shows a deformation band with closely spaced fringes corresponding to higher levels of stresses due to the plastic deformation.

4 ANALYSIS AND DISCUSSION

The plastic process of the three polymeric materials was investigated starting from the yielding point until the fracture event. The analysis for the yield strength is presented followed by a detailed comparison of the plastic response of the polymers for specific strains and the determination of a constitutive relation between the stress as a function of strain and strain rate.

4.1 Yielding an Cold Drawing Processes

The nominal stress vs. strain curves plotted in Figures 2, 3, and 4 show that the yield strength increases with strain rate for the three polymers while the nominal strain for yielding is constant for PC, and decreases slightly for PP and HDPE. The decrease in stress after the polymers yield corresponds to strain softening while the cold-drawing event is responsible of the strain hardening of the samples [8, 9, 36]. The relationship between the yield strength and the strain rate for the three polymers tested is shown in Figure 7. As expected, the graph shows a highest strength for the PC samples, followed by the PP and finally by the HDPE samples. Figure 7 shows that the yield strengths vary linearly with the logarithm of the strain rate in the range of crosshead speed tested. The values of the coefficients for the fitting equations are shown in Table 1.

Several authors have reported similar relations for the yield strength with strain rate for the polymers tested [1, 9, 36]. This relation is consistent with Eyring's equation, which establishes that the yield strength of polymers is related to the strain rate and temperature by the following equation:

$$\frac{\sigma_y}{T} = \left(\frac{\Delta U}{vT}\right) + \left({}^{R_G}\!/_{v}\right) \ln\left[\frac{2\dot{\varepsilon}}{e_o}\right]$$

where σ_y is the yield stress, T is the temperature of the test, ΔU the activation energy of plastic deformation, $\dot{\varepsilon}$ the strain rate, R_G the gas constant, v the activation volume of the element unit, and e_o the pre-exponential factor.

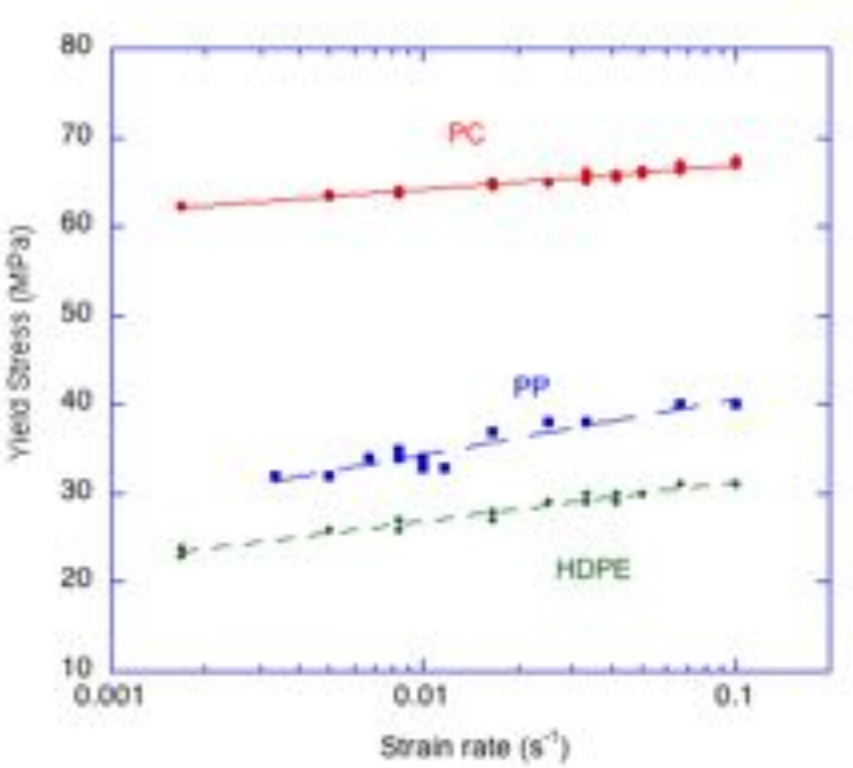

Figure 7: Yield strength vs. strain rate for PC, PP, and HDPE

It is important to note that for some glassy polymers such as PC, polymethylmethacrylate (PMMA), and polyvinylidene difluoride (PVDF) it has been reported a bilinear dependence of the yield stress with the logarithm of strain rate. However the change in slope of the linear relations has occurred at the high strain rates achieved with compressive or tensile Split Hopkinson Pressure Bar (SHPB) [4, 10, 30, 31].

Polymer	*A*	*B*	R
PC	69.56	2.68	0.98
PP	46.91	6.25	0.96
HDPE	35.77	4.42	0.98

$$\sigma_y = A + B\log(\dot{\varepsilon})$$

σ_y : Yield strength, MPa

$\dot{\varepsilon}$: Strain rate, s^{-1}

Table 1: Parameters for the fitting equation of yield strength vs. strain rate for PC, PP, and HDPE

The nominal, true and cold drawing stresses (as defined in the Materials and Experimental Method section) for a PC, and a PP samples tested at 15 mm/min are shown in Figure 8. The ratio between the final and initial cross section areas for the PC samples are approximately 1.5, for the PP 2.2, and for the HDPE 3.5 (not shown here). The actual stress on the sample section where the necking is propagating during the cold drawing event is approximately constant for PP while for PC increases steadily. The HDPE samples exhibit similar behaviour to the PP.

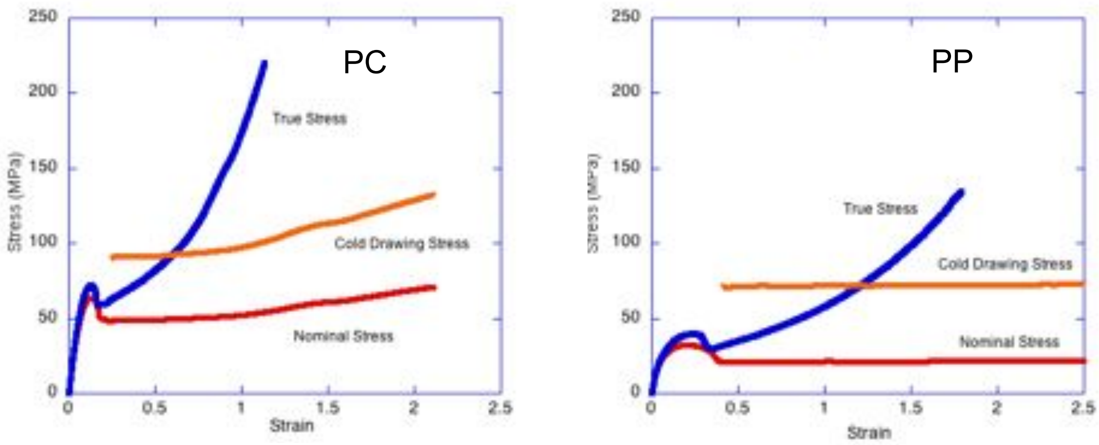

(a) (b)

Figure 8: Stress vs. strain for a strain rate of 15 mm/min.
(a) Polycarbonate, (b) Polypropylene.

Nominal stress/strain curves are based on the original cross section, true stress/strain curves are calculated using the actual area assuming incompressibility, and cold drawing stresses use the final cross area. The strains were calculated as displacement divided by initial gage length

Figure 9 displays a sequence of plots showing how the nominal stress varies with the crosshead speed for strains equal to 0.1, 0.2, 0.4, 0.7, and 1.75. These isostrain graphs were constructed using the nominal stress vs. strain curves obtained for each crosshead speed tested.

For a specific nominal strain the nominal stresses and corresponding crosshead speed of all tests were read and graphed. In the first plot, at strain equal to 0.1, all polymers are in the pre-yielding region. In the graph corresponding to 0.2 strain, a decrease can be observed in the PC while the PP and HDPE exhibit an increase. The reduction of the PC stresses corresponds to yielding that occurs at strains varying between 0.12 to 0.13. The PP and HDPE are still in the pre-yielding section.

The PP samples yield at strains that go from 0.2 to 0.14 as the strain rates increase, while the HDPE starts yielding at slightly higher strains, from 0.23 to 0.14. This difference in behavior is still displayed in the plot for strain equal to 0.4 where both polymers have already yielded and nevertheless the stresses on the PP samples are lower than the HDPE samples.

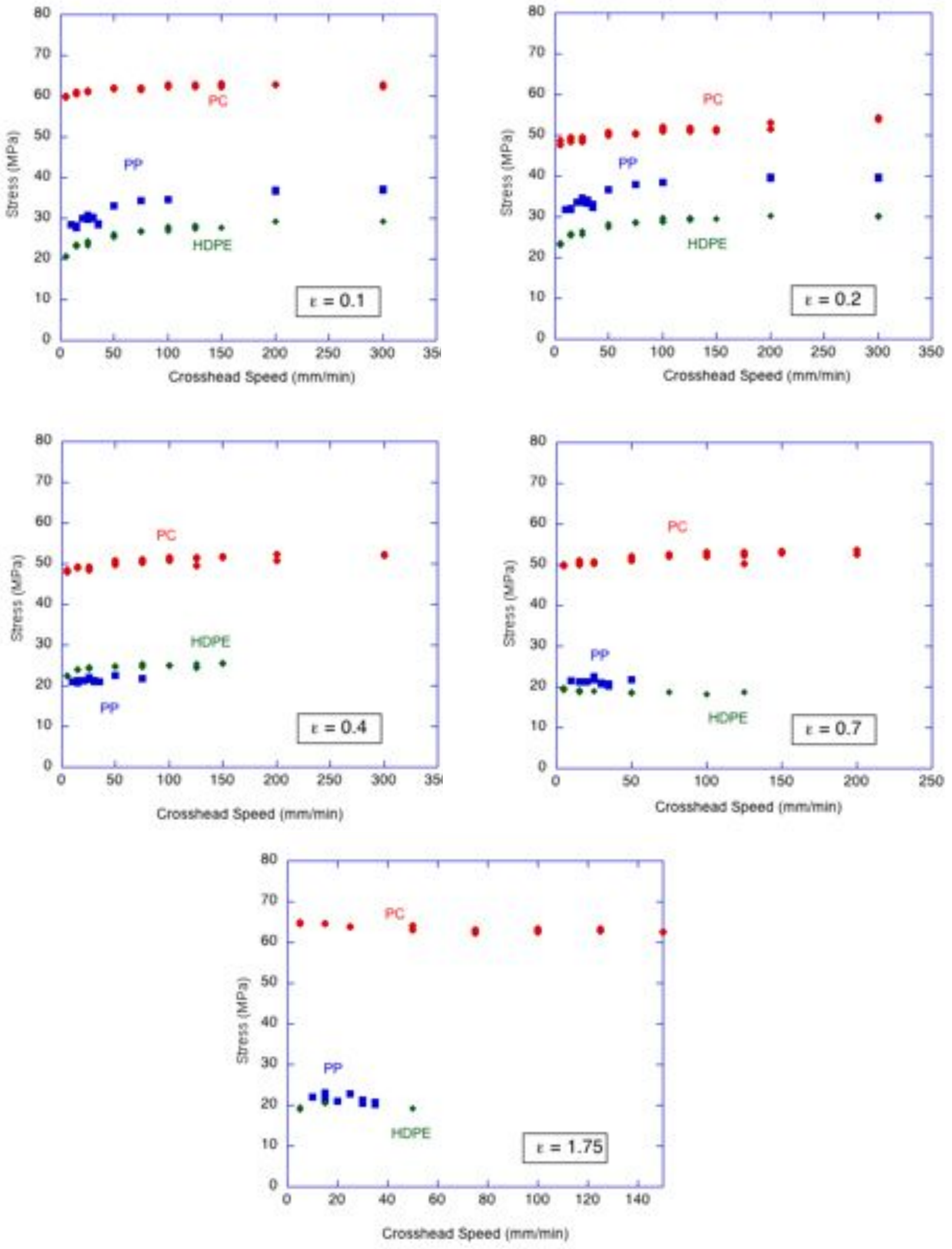

Figure 9: *Comparison between PC, PP, and HDPE behavior: isostrain curves showing nominal stress vs. crosshead speed for strains equal to 0.1, 0.2, 0.4, 0.7, 1.75*

At strain equal to 0.7, the PP stresses are slightly higher but at higher strains there is no difference between the two polymers as it is shown in the graph for strain equal to 1.75.

Summaries of the viscoplastic behavior of the three polymers for the range of crosshead speeds tested are displayed in Figures 10, 11 and 12 for particular strain values.

The graph for the PC in Figure 10 shows that the nominal stress changes as the crosshead increases. At crosshead speeds higher than 25 mm/min, the stress approaches a constant value, and thus depends primarily on the strain.

The PP and HDPE exhibit a very different behavior, as the strain increases a progressive decrease occurs until it reaches a plateau that corresponds to the propagation of the neck during the cold drawing event. Figure 11 shows that for the PP the strain at which this happens is close to 0.4. For the HDPE the post-yielding region extends up to strains equal to 0.6, whereas a well developed neck propagates for strains greater than 0.7 independently of the crosshead speed (see Figure 12).

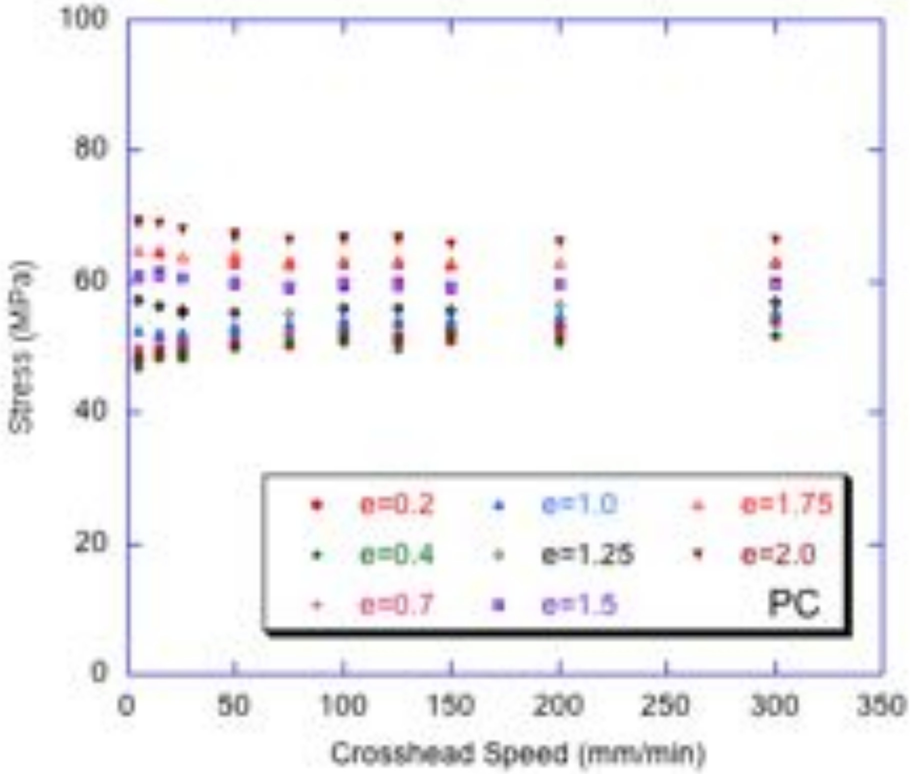

Figure 10: Nominal stress vs. Crosshead speed. Isostrain curves show the viscoplastic behavior of the polycarbonate.

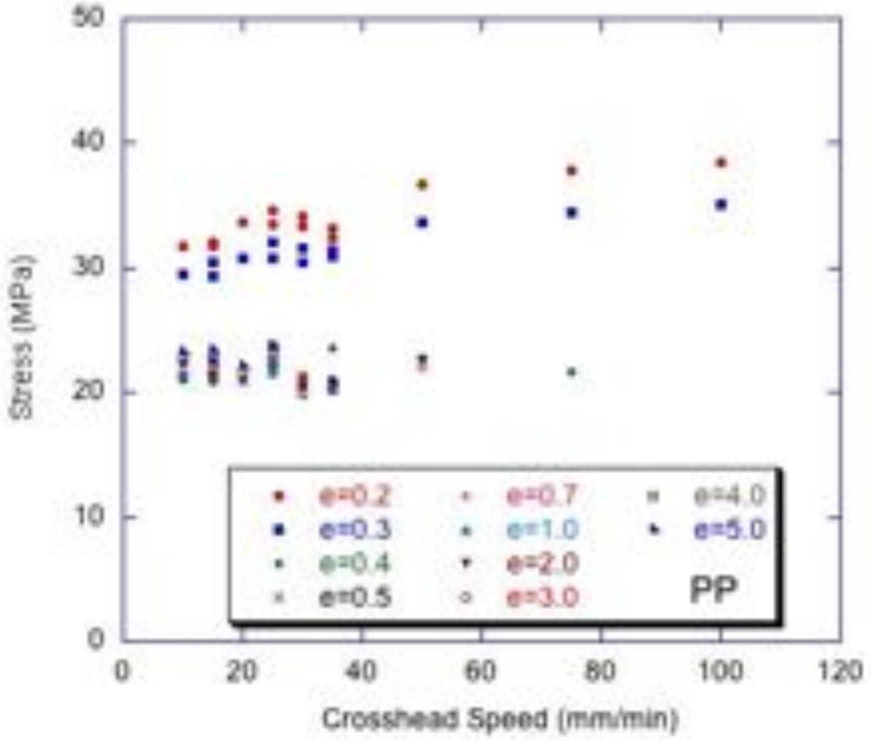

Figure 11: *Nominal stress vs. Crosshead speed. Isostrain curves show the viscoplastic behavior of the polypropylene.*

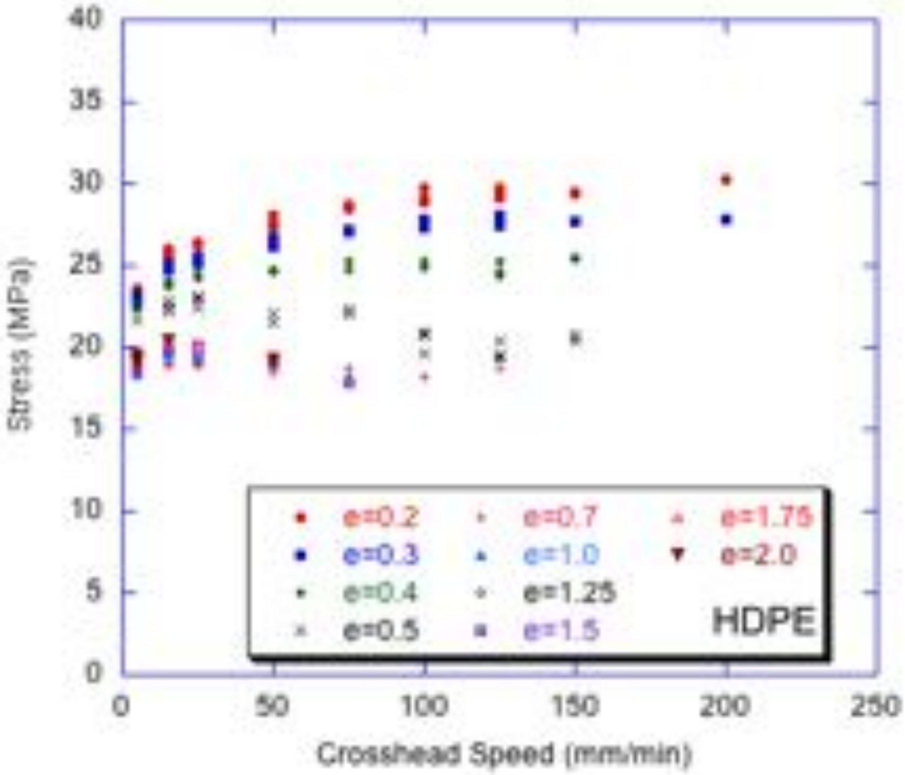

Figure 12: *Nominal stress vs. Crosshead speed. Isostrain curves show the viscoplastic behavior of the polypropylene.*

4.2 Determination of the Constitutive Equation

One of the goals of this work was to find a single constitutive equation $\sigma(\varepsilon, \dot{\varepsilon})$ to represent the viscoplastic deformation of the three polymeric materials investigated as a function of strain and strain rate. This would simplify a comparative analysis of viscoplastic behavior of the polymers under the same deformation process. Although the true stresses and strains measured while a constant true strain rate would represent the “real plastic flow” of the polymer while in tension, from a practical point of view the nominal stress-strain curves obtained with constant crosshead speed allows the user to assess and compare quickly the viscoplastic response of the polymers studied under similar conditions.

Two types of constitutive equations have been used to describe the relation between the stress, σ, the strain, ε, and the strain rate, $\dot{\varepsilon}$, for plastic deformation of metals and solid polymers. The first one is the multiplicative type [13, 26, 41] where the stress is expressed as the product of the strain and the strain rate as follows:

$$\sigma(\varepsilon, \dot{\varepsilon}) = f(\varepsilon) \cdot g(\dot{\varepsilon}) \tag{3}$$

In the second type, known as the additive type [41-43], the effect of the strain is added to the term representing the strain rate:

$$\sigma(\varepsilon, \dot{\varepsilon}) = f'(\varepsilon) + g'(\dot{\varepsilon}) \tag{4}$$

A multivariable non-linear least square fitting (NLSF) was used to fit the experimental data to several additive and multiplicative type equations. The non-linear regressions were performed using Origin 7.5 software, which is based on the Levenberg-Marquardt algorithm. Among other features this software allows to estimate initial values for the parameters, monitor the iterative process, and keep the value of the parameters fixed or variable.

Two constitutive laws used for metals were tested [41]. The first one was:

$$\sigma = K\left[\varepsilon^{n} + m \ln\left(\frac{\dot{\varepsilon}}{\dot{\varepsilon}_o}\right)\right] \tag{5}$$

This equation where the strain rate hardening term is added to the strain hardening term has been used successfully to describe the deformation of metals at room temperature. The second equation tested has been used for deformation of metals at high temperatures, and is expressed as the product of the power laws of the strain hardening and the strain rate as follow:

$$\sigma = K\varepsilon^{n}\dot{\varepsilon}^{m} \tag{6}$$

These constitutive laws did not give a good fit of the experimental data gathered in this work.

Another equation used was:

$$\sigma = k\exp\left(h\varepsilon^{2}\right)\left[\frac{\dot{\varepsilon}}{\dot{\varepsilon}_{o}}\right]^{m} \qquad (7)$$

where ε_o was a fixed strain reference value.

This constitutive law was used by Duffo et al [13] for PP, and G'Sell and Jonas [26] for HDPE. Both works report a strain hardening exponent equal to two. In the present work this equation fitted the PC and HDPE but not the PP data.

Additional equations were tried using the forms of equations 3 and 4, and the following expression gave the best fitting for the three polymers:

$$\sigma = \sigma_{o} + \gamma\dot{\varepsilon}^{m}\exp\left(n\varepsilon^{k}\right) \qquad (8)$$

where $\sigma =$ nominal stress (MPa), $\sigma_o =$ independent strength coefficient, $\dot{\varepsilon} =$ strain rate (s^{-1}), $\varepsilon =$ nominal strain, $\gamma, m =$ strain rate hardening coefficient and exponent, $n, k =$ strain hardening coefficient and exponent.

The values of the fitting parameters, their corresponding errors, and the R^2 for each fitting are shown in Table 2. The fitting equations and the experimental data for the polymers were graphed in Figures 13, 14, and 15. In the case of the PP several fittings with different parameters where found, the one chosen for this work was obtained with the *k* parameter equal to 10 to obtain the smallest errors and R^2. For the PC, this equation fits the experimental data at crosshead speeds greater than 25 mm/min where the stress depends primarily on strain.

Polymer	γ	**m**	**n**	σ_o (MPa)	**k**	**R^2**
PC	52.02±0.23	0.01±0.001	0.07±0.003	0	2.05±0.06	0.96
PP	27.78±1.10	0.17±0.01	-54,997±3,229	21.57±0.09	10	0.97
HDPE	17.03±0.71	0.17±0.01	-25.21±5.41	19.24±0.09	4.18±0.27	0.96

Table 2: Fitting parameters and correlation for the constitutive equations for PC, PP, and HDPE.

The term $\dot{\varepsilon}^{m}$ represents the strain rate sensitivity of the material as a power law, while the term $\exp(n\varepsilon^{k})$ takes into account the strain hardening contribution at large deformations. The single constitutive relation derived for the polymeric materials describes the viscoplastic response of all three polymers studied for crosshead displacements from 25 to 300 mm/min and strains up to the fracture events. This unified model facilitates its implementation for computer simulations of polymer processing. The relation found in this study applies only to constant strain rate uniaxial tensile test at room temperature in the range of 0.01 to 0.1 s^{-1} strain rates. This relation does not incorporate previous deformation histories of the materials.

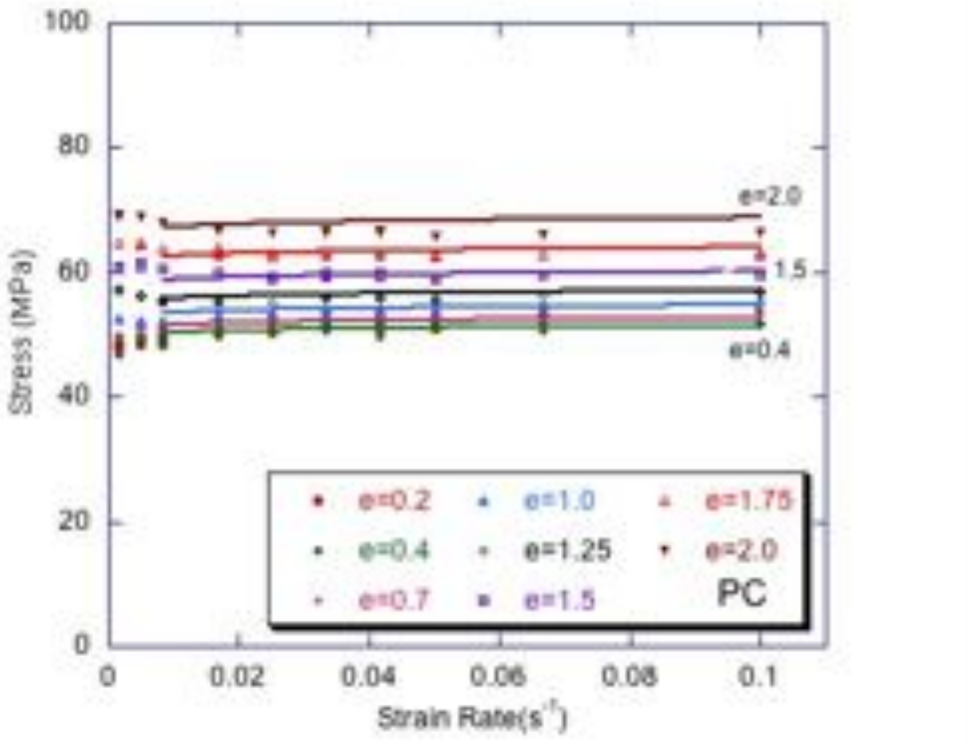

Figure 13: Nominal stress vs. Strain rate (Fitting curves and experimental data for polycarbonate).

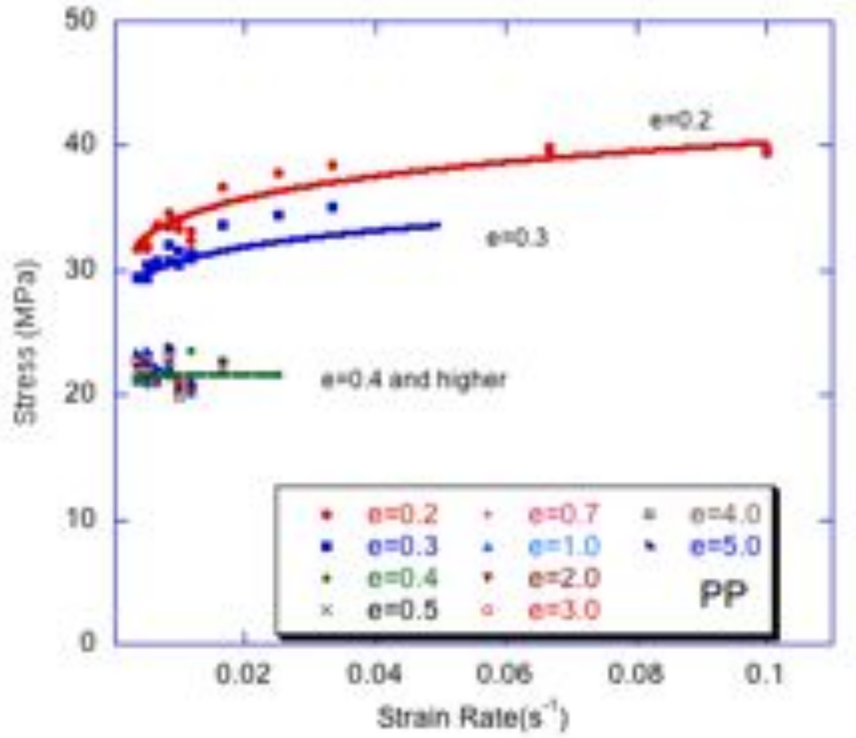

Figure 14: Nominal stress vs. Strain rate (Fitting curves and experimental data for polypropylene).

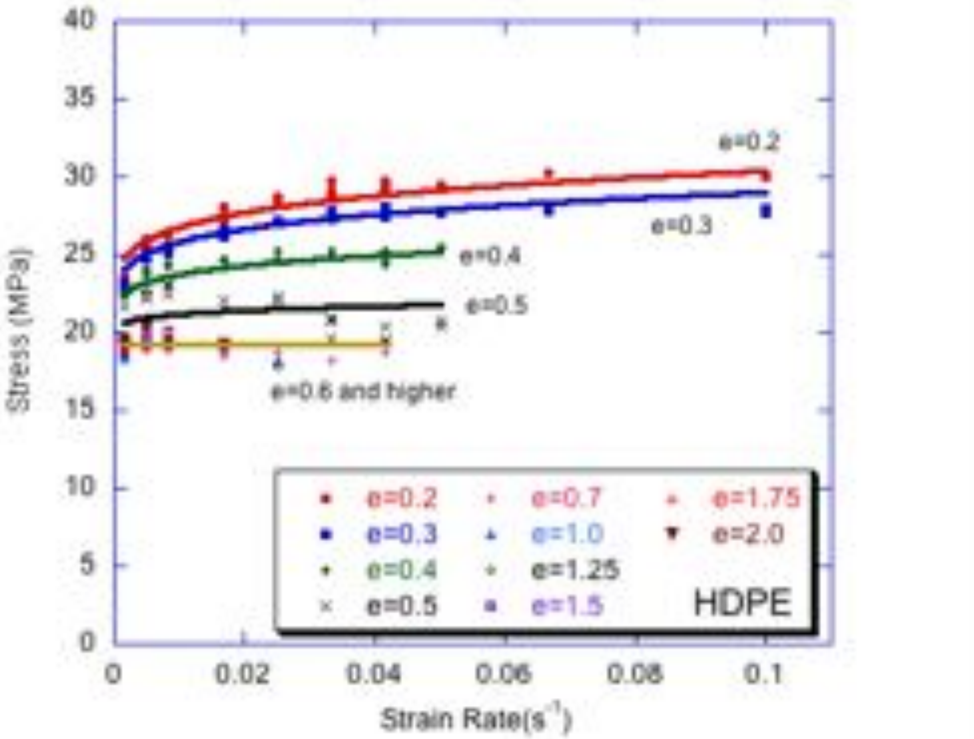

Figure 15: Nominal stress vs. Strain rate (Fitting curves and experimental data high density polyethylene).

5 CONCLUSIONS

Uniaxial tensile tests at constant crosshead displacement rates and large strains were performed on polycarbonate, polypropylene, and high density polyethylene samples at room temperature. The yield strength increases with strain rate for the three polymers while the nominal strain for yielding is constant for PC, and decreases slightly for PP and HDPE. Two models were developed that describe the behavior of all three materials similar to that shown in prior work; an Eyring equation is used to describe the yield behavior. Furthermore, a single constitutive equation is developed in this work for $\sigma(\varepsilon,\dot{\varepsilon})$ to represent the plastic deformation of the three polymeric materials as a function of strain and strain rate in the range of 0.01 to 0.1 s^{-1} strain rates.

6 ACKNOWLEDGEMENTS

The authors acknowledge the funding support of the National Defense Science and Engineering Graduate fellowship (NDSEG), the University of Puerto Rico at Mayaguez, from where B. Calcagno is on leave of absence, Dan Morgan for his help with the figures, and Alejandro Londoño for his help with the injection molding process.

7 REFERENCES

[1] Drozdov, A.D.; Christiansen, J.D. The effect of strain rate on the viscoplastic behavior of isotactic polypropylene at finite strains
Polymer, 2003. 44(4): p. 1211-1228

[2] Osswald, T.A.; Brinkmann, S.; Oberbach, K, et. al International Plastics Handbook
Hanser Publishers, 2006: p. 522, 538, 600

[3] Osswald, T.A.; Hernández-Ortíz, J.P. Polymer Processing: Modeling and Simulation
Hanser Publishers, 2006: p. 30

[4] Mulliken, A.D.; Boyce, M.C. Mechanics of the rate-dependent elastic-plastic deformation of glassy polymers from low to high strain rates
International Journal of Solids and Structures, 2006. 43(5): p. 1331-1356

[5] Callister, W.D. Materials Science and Engineering An Introduction.
Wiley, 2003: p. 481-488

[6] T.L., Anderson Fracture Mechanics Fundamental and Applications
CRC, 2005: p. 260-281

[7] Ehrenstein, G.W. Polymeric Materials: Structure - Properties – Applications
Hanser Publishers, 2001: p. 167-225

[8] Arruda, E.M.; et al. Rate dependent deformation of semi-crystalline polypropylene near room temperature
Journal of Engineering Materials and Technology-Transactions of the ASME, 1997. 119(3): p. 216-222

[9] Dasari, A.; Misra, R.D.K. On the strain rate sensitivity of high density polyethylene and polypropylenes. Materials Science and Engineering a-Structural Materials Properties Microstructure and Processing, 2003. 358(1-2): p. 356-371

[10] Sarva, S.S.; Boyce, M.C. Mechanics of polycarbonate during high-rate tension. Journal of Mechanics of Materials and Structures, 2007. 2(10): p. 1853-1880

[11] Boyce, M.C.; Arruda, E.M. An Experimental and Analytical Investigation of the Large Strain Compressive and Tensile Response of Glassy-Polymers. Polymer Engineering and Science, 1990. 30(20): p. 1288-1298

[12] Drozdov, A.D.; Christiansen, J.D. Thermo-viscoelastic and viscoplastic behavior of high-density polyethylene. International Journal of Solids and Structures, 2008. 45(14-15): p. 4274-4288

[13] Duffo, P.; et al. Rheology of Polypropylene in the Solid-State. Journal of Materials Science, 1995. 30(3): p. 701-711

[14] Duan, Y.; et al. A uniform phenomenological constitutive model for glassy and semicrystalline polymers. Polymer Engineering and Science, 2001. 41(8): p. 1322-1328

[15] Ward, I.M. The Mechanical Properties of Solid Polymers. Wiley, 2004: p. 83-88; 241-250

[16] Lakes, R. Viscoelastic Materials. Cambridge University Press, 2009: p. 1-10; 156-188

[17]	Seguela, R.	On the natural draw ratio of semi-crystalline polymers: Review of the mechanical, physical and molecular aspects Macromolecular Materials and Engineering, 2007. 292(3): p. 235-244
[18]	Osswald, T.A.; Menges, G.	Materials Science of Polymers for Engineers Hanser Publishers, 2003: p. 459-463
[19]	Dasari, A.; Duncan, S.J.; Misra, R.D.K.	Atomic force microscopy of plastically deformed polyethylene subjected to tensile deformation at varying strain rates Materials Science and Technology, 2002. 18(6): p. 685-690
[20]	Addiego, F.; et al.	Characterization of volume strain at large deformation under uniaxial tension in high-density polyethylene Polymer, 2006. 47(12): p. 4387-4399
[21]	Gsell, C.; Gopez, A.J.	Plastic Banding in Glassy Polycarbonate under Plane Simple Shear Journal of Materials Science, 1985. 20(10): p. 3462-3478
[22]	Lefebvre, J.M.; Escaig, B.	Plastic-Deformation of Glassy Amorphous Polymers - Influence of Strain Rate Journal of Materials Science, 1985. 20(2): p. 438-448
[23]	Fleck, N.A.; Stronge, W.J.; Liu, J.H.	High Strain-Rate Shear Response of Polycarbonate and Polymethyl Methacrylate Proceedings of the Royal Society of London Series a-Mathematical Physical and Engineering Sciences, 1990. 429(1877): p. 459-&
[24]	Arruda, E.M.; Boyce, M.C.; Jayachandran, R.	Effects of Strain-Rate, Temperature and Thermomechanical Coupling on the Finite Strain Deformation of Glassy-Polymers Mechanics of Materials, 1995. 19(2-3): p. 193-212

[25] Pandermarakis, Z.G.; Spathis, G. An homogenization procedure for the description of pre- and post-yielding stages of isotropic polymer composites

Polymer Composites, 2008. 29(9): p. 978-991

[26] Gsell, C.; Jonas, J.J. Determination of the Plastic Behavior of Solid Polymers at Constant True Strain Rate

Journal of Materials Science, 1979. 14(3): p. 583-59

[27] Drozdov, A.D.; Christiansen, J.D.C. Finite viscoplasticity of semicrystalline polymers

Archive of Applied Mechanics, 2003. 72(10): p. 779-803

[28] Holmes, D.W.; Loughran, J.G. Theoretical aspects of the testing of elasto-viscoelastic-viscoplastic materials

Polymer Testing, 2008. 27(2): p. 189-203

[29] Walley, S.M.; et al. The Rapid Deformation-Behavior of Various Polymers

Journal De Physique Iii, 1991. 1(12): p. 1889-1925

[30] Siviour, C.R.; et al. The high strain rate compressive behaviour of polycarbonate and polyvinylidene difluoride

Polymer, 2005. 46(26): p. 12546-12555

[31] Siviour, C.R.; et al. Mechanical behaviour of polymers at high rates of strain

Journal De Physique Iv, 2006. 134: p. 949-955

[32] Boyce, M.C.; Parks, D.M.; Argon, A.S. Large Inelastic Deformation of Glassy-Polymers .1. Rate Dependent Constitutive Model

Mechanics of Materials, 1988. 7(1): p. 15-33

[33] Gsell, C.; Jonas, J.J. Yield and Transient Effects During the Plastic-Deformation of Solid Polymers

Journal of Materials Science, 1981. 16(7): p. 1956-1974

[34] Gsell, C.; et al. Video-Controlled Tensile Testing of Polymers and Metals Beyond the Necking Point
Journal of Materials Science, 1992. 27(18): p. 5031-5039

[35] Drozdov, A.D.; Christiansen, J.D. Viscoelasticity and viscoplasticity of semicrystalline polymers: Structure-property relations for high-density polyethylene
Computational Materials Science, 2007. 39(4): p. 729-751

[36] Kontou, E.; Farasoglou, P. Determination of the true stress-strain behaviour of polypropylene
Journal of Materials Science, 1998. 33(1): p. 147-153

[37] Spathis, G.; Kontou, E. Experimental and theoretical description of the plastic behaviour of semicrystalline polymers
Polymer, 1998. 39(1): p. 135-142

[38] ASTM D 1238 Standard Test Method for Melt Flow Rates of Thermoplastics by Extrusion Plastometer
ASTM International, 2004

[39] Murasawa, G.; Tohgo, K.; Ishii, H. Deformation behavior of NiTi/polymer shape memory alloy composites - Experimental verifications
Journal of Composite Materials, 2004. 38(5): p. 399-416

[40] ASTM D 638 Standard Test Method for Tensile Properties of Plastics
ASTM International, 2008

[41] Ghosh, A.K. Numerical-Analysis of Tensile Test for Sheet Metals
Metallurgical Transactions a-Physical Metallurgy and Materials Science, 1977. 8(8): p. 1221-1232

[42] Andrews, J.M.; Ward, I.M. Cold-Drawing of High Density Polyethylene
Journal of Materials Science, 1970. 5(5): p. 411

[43] Bauwensc.C.; Ots, J.M.; Bauwens, J.C. Strain-Rate and Temperature-Dependence of Yield of Polycarbonate in Tension, Tensile Creep and Impact Tests. Journal of Materials Science, 1974. 9(7): p. 1197-1201

Keywords:
viscoplastic behavior, polycarbonate, polypropylene, high-density polyethylene, plastic deformation

Stichworte:
viskoplastisches Verhalten, Polycarbonat, Polypropylen, Polyethylen hoher Dichte, plastische Verformung

Author/Autor:
Prof. Barbara O. Calcagno
Prof. Dr. Roderic Lakes
Prof. Dr. Tim Osswald
Prof. Dr. Wendy Crone*

E-Mail: barbara.calcagno@upr.edu
E-Mail: crone@engr.wisc.edu
Phone.: +1/608 262 8384
Fax: +1/608 263-7451

*Department of Engineering Physics
University of Wisconsin-Madison
543 Engineering Research Building
1500 Engineering Drive
Madison, WI 53706-1687

Editor/Herausgeber:
Europe/Europa
Prof. Dr.-Ing. Dr. h.c. G. W. Ehrenstein, verantwortlich
Lehrstuhl für Kunststofftechnik
Universität Erlangen-Nürnberg
Am Weichselgarten 9
91058 Erlangen
Deutschland
Phone: +49/(0)9131/85 - 29703
Fax.: +49/(0)9131/85 - 29709
E-Mail: ehrenstein@lkt.uni-erlangen.de

The Americas/Amerikas
Prof. Dr. Tim A. Osswald, responsible
Polymer Engineering Center, Director
University of Wisconsin-Madison
1513 University Avenue
Madison, WI 53706
USA
Phone: +1/608 263 9538
Fax.: +1/608 265 2316
E-Mail: osswald@engr.wisc.edu

Publisher/Verlag:
Carl-Hanser-Verlag
Jürgen Harth
Ltg. Online-Services & E-Commerce,
Fachbuchanzeigen und Elektronische Lizenzen
Kolbergerstrasse 22
81679 Muenchen
Phone.: 089/99 830 - 300
Fax: 089/99 830 - 156
E-mail: harth@hanser.de